RSC Advances

This article can be cited before page numbers have been issued, to do this please use: D. Sivakumar, K. M. Surapaneni, P. C. Prabu, N. Hari, P. Thiruvasagam, M. Rajasekaran and T. Sivaraman, *RSC Adv.*, 2015, DOI: 10.1039/C5RA23005E.

ROYAL SOCIETY OF CHEMISTRY

www.rsc.org/advances

View Article Online
DOI: 10.1039/C5RA23005E

Evaluation of the anticancer properties of the predicted hBaxBH3-mimetic compound 2-hydroxy-3,5-dinitrobenzamide in a mammary carcinogenesis-induced rat model

Dakshinamurthy Sivakumar[a], Krishna Mohan Surapaneni[b], Ponnachipudhur Chinnaswamy Prabu[c], Natarajan Hari[d], Ponnusamy Thiruvasagam[d], Muthu Rajasekaran[e] and Thirunavukkarasu Sivaraman[a]*

[a]Structural Biology Lab, Department of Bioinformatics, School of Chemical and Biotechnology, SASTRA University, Thanjavur – 613 401, Tamil Nadu, India.

[b]Department of Biochemistry, Saveetha Medical College & Hospital, Saveetha University, Chennai, Tamil Nadu, India.

[c]Central Animal Facility, SASTRA University, Thanjavur – 613 401, Tamil Nadu, India.

[d]Department of Chemistry, [e]Department of Biotechnology, School of Chemical and Biotechnology, SASTRA University, Thanjavur – 613 401, Tamil Nadu, India.

*To whom correspondence should be addressed.

Tel: +91 4362 264101 Ext.2319

Fax: +91 4362 264120

E-mail: sivaram@scbt.sastra.edu

View Article Online
DOI: 10.1039/C5RA23005E

Abstract

Designing small molecular prototypes having potential to disrupt binding interfaces of pro-apoptotic – anti-apoptotic/BH3-only proteins is a promising strategy in cancer chemotherapy. Several natural and synthetic chemical compounds have been reported as inhibitors or BH3-mimetics to anti-apoptotic proteins of the Bcl-2 family playing essential roles in apoptosis. In the present study, chemical synthesis, structural characterizations and anti-cancer effect of 2-hydroxy-3,5-dinitrobenzamide (HDNB), a chemical compound identified on the basis of pharmacophoric features of hBaxBH3 peptide have been systematically reported. Chemopreventive effect of the HDNB was assessed on N-Nitroso-N-methylurea-induced Wistar female rats of mammary gland carcinogenesis for the study period of 18 weeks. The carcinogenesis Wistar rats were subjected to oral administration of low-dose (8 mg/kg b.w.), medium-dose (40 mg/kg b.w.) and high-dose (200 mg/kg b.w.) of the HDNB in three different experimental setups. Strikingly, medium-dose (40 mg/kg b.w.) of the HDNB showed appreciable potential to reverse the abnormalities of various biochemical parameters in blood samples and as well in breast tissues to the values as close as to that of healthy control or to that of standard (Tamoxifen) control. The chemopreventive potential of the HDNB could be chiefly attributed to its ability of restoring antioxidants and as well apoptosis inducing properties in Wistar animal models.

Key words: Acute toxicities; anti-cancer potential; apoptotic proteins; breast cancer; chemo preventive; HDNB.

View Article Online
DOI: 10.1039/C5RA23005E

1. Introduction

Cancer is caused by uncontrolled cell proliferations and as well by abnormally increased cell life due to defects in apoptosis.[1] The two processes are governed by quite a large number of parallel signaling pathways, which posits great challenges on designing target-based small molecular therapeutic agents to the treatments of cancers.[2, 3] Fortunately, many anticancer compounds have been shown to regulate apoptotic machinery in one way or other in order to combat cancerous cells.[4, 5] In these contexts, designing lead compounds depicting desirable effects by interfering functions of Bcl-2 family proteins has become an attractive strategy in cancer chemotherapy.[6] Though it is well documented that Bcl-2 family proteins tightly govern the apoptotic process by intrinsic or mitochondrial pathway, the mechanism by which the proteins communicate each other and modulate the process are under debate between two key models: direct activation model and indirect model.[7-9] The 'direct activation model' proposes that pro-apoptotic proteins (Bax and Bak) will be activated by a set of BH3-only proteins (Bim, Bid and Puma), which may be abnormally sequestered by anti-apoptotic proteins (Bcl-2, Bcl-B, Bcl-W, Bcl-XL, Bfl-1 and Mcl-1) in cancerous cells, whereas 'indirect model' proposes that functions of pro-apoptotic proteins will be blocked by anti-apoptotic proteins through hetero-complex formations between the two groups of the Bcl-2 family. Interestingly, both models suggest that chemical molecules that are capable of acting as antagonists to the anti-apoptotic proteins can act as efficient lead anti-cancer compounds, in general.

Impairment in apoptosis is one of hallmarks of cancer diseases and successively overexpression of anti-apoptotic proteins (either all or a few of them) have been documented in most types of cancers, if not all.[10] To date, six types of anti-apoptotic proteins have been well characterized in mammalian cells and all the proteins have similar three-dimensional (3D)

View Article Online
DOI: 10.1039/C5RA23005E

architectures. However, biological activities and as well specificities of the anti-apoptotic proteins to interact with various BH3-only proteins are not identical to each other. Many natural products (antimycin A, chelerythrine, obatoclax, purpurogallin and gossypol) and synthetic chemical compounds (HA14-1, BH3I-1, isooxazolidine derivatives, gossypol derivatives, ABT-737 and ABT-263) have been reported as inhibitors to the anti-apoptotic proteins and compounds such as ABT-263, obatoclax, gossypol and isooxazolidine are right now under various levels of clinical trials.[4] Interestingly, of the many molecules mentioned above, the ABT-737 and ABT-263 have only been authenticated as true antagonists/BH3-mimetics to the anti-apoptotic proteins as cytotoxic activities of the compounds could be well correlated with cellular concentrations of the anti-apoptotic proteins.[4, 11, 12] Moreover, structural interactions of the compounds with Bcl-2/Bcl-XL have also been well studied at atomic level resolutions.[11] However, the two compounds were found to be weak antagonists to Mcl-1 and as well the compounds were inactive against cancerous cells over-expressing the anti-apoptotic protein, Mcl-1.[13] Ostensibly, designing/identifying specific antagonists to each anti-apoptotic protein and likewise common antagonists showing high affinities to all of the 6 anti-apoptotic proteins have been yet challenging tasks in cancer chemotherapy.

We have recently reported 2-hydroxy-3,5-dinitrobenzamide (HDNB) as a lead inhibitor to human Bcl-B (hBcl-B) by means of peptidodynmimetic method designed in our laboratory.[14] The method is useful to define pharmacophoric features of small peptides bound with large protein molecules under dynamic conditions. Using the peptidodynmimetic method, pharmacophoric residues of human Bax-BH3 (hBax-BH3) peptide bound with hBcl-B were mapped out and the HDNB was identified as novel lead inhibitor to the hBcl-B upon a database screening followed by high throughput virtual screening on the basis of the pharmacophoric

View Article Online
DOI: 10.1039/C5RA23005E

residues of the hBax-BH3. Interestingly, the lead compound (HDNB) also showed comparable binding affinities on the BH3-binding grooves of all the anti-apoptotic proteins but with Bcl-W, appreciable bioavailability and desirable pharmacokinetic properties as predicted by using an array of computational strategies.[14, 15] In the present study, we report chemical synthesis, structural characterizations (using ultraviolet visible (UV) spectroscopy, Fourier transform infrared (FT-IR) spectroscopy, Gas chromatography - mass spectrometry (GC-MS) and proton (^{1}H), carbon (^{13}C) and nitrogen (^{15}N) nuclear magnetic resonance (NMR) spectroscopy) and chemopreventive potential of the HDNB in N-Nitroso-N-methylurea (NMU) - induced Wistar mammary gland carcinogenesis in detail. Comprehensive analyses of data obtained from the experiments suggested that the HDNB is a promising lead depicting anti-cancer potential and the HDNB would also be perhaps used as a seed molecule to develop highly efficient *de novo* antagonists to the anti-apoptotic proteins.

2. Results and Discussion

Understanding relationships between small bio-molecules and macromolecules synthesized by cells is crucial to make 'central dogma' of life to be entirely descriptive one. Natural and non-natural small chemical molecules are also key elements, powerful probes and drugs in biological systems.[16, 17] In these connections, designing small molecules having potential especially to disrupt protein – protein interfaces has intrigued researchers in the past decade. However, designing/identifying chemical molecules binding to protein-protein interfaces is an uphill task as surface areas of the interfaces are large and flat, in general.[18, 19] Interestingly, hotspots (subset of residues contributing most of the free energy of binding) of proteins constituting interfaces could be mapped out by using site-directed mutational studies as demonstrated for several proteins.[20] The hotspots of the proteins could be used as 'footholds' for

View Article Online
DOI: 10.1039/C5RA23005E

designing of small molecules interacting on the interfaces of protein complexes. Computational methods such as fragment-based lead designing and peptidomimetics have also been shown as promising strategies for designing leads to interact on protein-protein interfaces.[21] In these series of *in silico* tools, a recent peptidodynmimetic method has also been shown to define pharmacophoric residues of the hBaxBH3 bound with hBcl-B under dynamic conditions.[14] Using the pharmacophoric residues of the peptide, MMsINC database (as represented in the original article[22]) consisting of 17 million conformers of about 4 million diverse molecules was screened through pepMMsMIMIC interface in order to identify lead chemical compounds mimicking the interaction of the hBaxBH3 on the BH3-binding groove of the hBcl-B.[14, 22] After subjecting a few hundred compounds screened using the 'peptododynmimetic strategy' to high throughput virtual screening followed by pharmacokinetic evaluations, the HDNB was identified as a prototypic chemical molecular inhibitor to the hBcl-B. Furthermore, binding affinities of the HDNB towards the 6 anti-apoptotic proteins from human beings have also been recently scrutinized by means of *in silico* methods and differential binding modes of the HDNB with the anti-apoptotic proteins could be chiefly attributed to differences in the chemical properties of BH3-binding grooves of the proteins.[15]

2.1 Synthesis and structural characterizations of the HDNB

The HDNB was not commercially available during course of the present studies and even till now. Synthetic methodology of the HDNB is outlined in Figure S1 and also described in the 'Method' section. Structural characterizations of the HDNB as examined by UV, FT-IR and GC -MS spectrometric techniques have been elaborately delineated in the supplementary material (Figure S2 and Table S1) and comprehensive analyses of the data could consistently represent the structure of the HDNB. In addition, elemental composition of the HDNB ($C_7H_5N_3O_6$) as

View Article Online
DOI: 10.1039/C5RA23005E

determined by using 2400 series CHNS Elemental analyzer (PerkinElmer, Wellesley, USA) were in good agreement with elemental composition of the compound calculated out theoretically: percentage compositions of C, H & N were 34.87%, 2.50% & 16.95% respectively, as determined by the experimental method and the theoretic values were 37.02%, 2.22% & 18.50% respectively, for the elements. Moreover, nuclear magnetic frequencies of protons, carbons and nitrogen present in the compound were also recorded using various 1D and 2D NMR methods. 1D ^{1}H NMR spectra of the 3,5-dinitiro salicylic acid (DNSA, the starting compound) and HDNB are shown in Fig. 1A and 1B, respectively. The DNSA showed two dispersed resonances at δ 8.67 and δ 8.71 for aromatic protons located at 4th and 6th positions, respectively and phenolic OH resonance of the compound was observed as a weakly resolved peak at δ 9.0. The HDNB also showed two peaks for its aromatic protons at δ 8.65 and δ 8.70. In addition, the compound showed three sharp singlet resonances at δ 7.04, δ 7.21 & δ 7.38 and a weak broadened peak at δ 14.16. The former and later resonances were assigned to protonated amide group ($CONH_3^+$) and phenolic OH group of the compound. The resonance assignments were further authenticated by acquiring 1D ^{1}H NMR for the HDNB for which labile protons could be exchanged to solvent deuterium and the deuterated HDNB showed two ^{1}H resonances for its two non-labile aromatic protons only (Fig. 1C). Moreover, Distortionless Enhancement by Polarization Transfer (DEPT) experiments carried out for the HDNB is shown in Fig. 1D and the data depicted two ^{13}C resonances at δ 125.9 and δ 131.5 indicating that the compound has only two tertiary carbon atoms (C4 and C6, which are free of substitutions in the aromatic ring). Thus, the DEPT and 1D ^{1}H NMR data on the HDNB endorsed each other and confirmed the resonance assignments. We also performed 2D Heteronuclear Single Quantum Correlation (HSQC) - ^{15}N experiments for the HDNB and the data is shown in Fig. 1E. The HSQC spectrum depicted a single cross peak at δ

View Article Online
DOI: 10.1039/C5RA23005E

358.1 of ^{15}N dimension and δ 7.18 of ^{1}H dimension confirming the presence of an amide group in the compound. Taken together, the data presented above could unambiguously confirm the structure of the HDNB as represented in the Fig. S1.

2.2 Acute oral toxicity (AOT) studies on the HDNB

The HDNB consists of two nitro groups, which could rise up skeptical concerns on toxicity and adverse effects of the compound in human system. Since compounds consisting of nitro groups become electrophilic in nature, it is generally considered that the nitro compounds may cause some deleterious changes by interacting with biological nucleophilic molecules such as nucleic acids and proteins.[23] Unless until the nitro compounds damage healthy normal cells, they may be of safe to use as drugs in the human system. Interestingly, several drugs with nitro groups are already in market. For instance, drugs such as chloramphenicol (as an antibiotic), nitrazepam (as a tranquilizer), pyrrolnitrin (as fungicide), nitridazole (as schistosonicide), parathion (as insecticide) and azathioprine (as antineoplastic) are popular examples for the category of the compounds.[23] In addition, ABT-737, a well-known antagonist to anti-apoptotic proteins, has a nitro group and the compound is right now under Phase I clinical trials.[4] However, toxicities of small chemical molecules are not predictable in a straightforward manner, since about 40% of lead molecules fail either in pre-clinical or clinical trials as suggested by recent surveys on toxicities of small molecules.[24, 25] In these backgrounds, irrespective of literature evidences on non-toxic/toxic properties of compounds possessing nitro group(s), we have thoroughly evaluated toxicity of the HDNB by using female Wistar rats.

As per OECD (Organization for Economic Cooperation and Development) 425 guidelines (OECD, 2001), 'Main test' (5 Wistar female rats were used in the test: first and second rats were administrated with 175 mg/kg b.w. and 550 mg/kg b.w., respectively; other

View Article Online
DOI: 10.1039/C5RA23005E

three rats were administrated with 2000 mg/kg b.w.) procedure was strictly followed to determine 'lethal dose' (LD_{50}) of the HDNB. All the 5 rats treated with various doses of the HDNB were periodically monitored for 14 days from the treatments and the HDNB-treated animals did not develop any toxicity signs such as tremors, convulsions, salivation, diarrhea, lethargy, sleep and coma. Only the animals administrated with 2000 mg/kg b.w. seemed to be lethargic in the first 20 minutes of treatment periods and thereafter they become active as healthy animals. All the five HDNB-treated Wistar rats survived AOT time span of 14 days and at completion of the treatment periods, all the 5 Wistar rats were sacrificed and subjected to detailed necropsy studies. Fig. 2 shows histopathology of different organs (such as brain, heart, lung, liver, kidney and intestine) of the Wistar female rats treated with 2000 mg/kg b.w. of the HDNB. Examination on the histology of the organs suggested that there were no abnormal or pathological changes due to oral administration of the HDNB to the test animals: cerebral/cerebellar hemispheres of brains, myocytes of heart section and hepatocytes of liver were characterized to be as normal as in the healthy rats; lung section showed normal alveolar / bronchiolar epithelium with no infiltrates; kidney section showed the normal cortex and medulla with glomeruli and tubules showing their normal micro-architecture; there were no necrotic lesions of the epithelium in the intestinal section.[26, 27] Thus, the AOT studies revealed that the HDNB administrated orally to the Wistar rats was not toxic at dose level of 2000 mg/kg b.w. and LD_{50} of the compound should also be at least greater than 2000 mg/kg b.w.

2.3 Chemopreventive effect of the HDNB using animal models

2.3.1 Cancer induction and treatment

Chemopreventive effect of the HDNB was tested on breast cancer animal models on the basis of results obtained from *in vitro* MTT (3-[4,5-dimethylthiazol-2-yl]2,5-diphenyltetrazolium

View Article Online
DOI: 10.1039/C5RA23005E

bromide) assays carried out for the HDNB. Cell growth inhibition potential of the HDNB was examined against MCF-7 (human breast cancer cells), HeLa (cervical cancer cells) and MG-63 (human osteosarcoma cells) cell lines and results of the assays are shown in Fig. 3. The cell lines were treated with various concentrations of the HDNB at constant treatment time of 48 h (Materials and Methods). By fitting the dose-dependent inhibition potential of the HDNB against growth of the cell lines to an appropriate non-linear regression reveled that IC_{50} values of the HDNB against MCF-7, MG-63 and HeLa cell lines were 574 ± 3 μM, > 2 mM and > 5 mM, respectively. The MTT assay suggested that the HDNB strongly inhibited growth of breast cancer cells than that of bone/cervical cancer cells used in the study. Hence, chemopreventive effect of the HDNB on NMU-induced breast cancer animal models was examined using 42 female Wistar rats for the time span of 18 weeks. The experimental animals were divided into 7 groups with 6 animals in each group (Table 1): control group, vehicle group, diseased group, standard group and 3 HDNB-treated groups (groups treated with low, medium and high doses of the HDNB were denoted as low-dose group, medium-dose group and high-dose group, respectively). The animals of the control group and vehicle group received only normal saline (1 ml) and corn oil (1 ml) as treatment doses, respectively, every alternative day throughout the experimental period. The breast cancer inductions and treatments were started simultaneously by administrating the NMU at concentration 75 mg/kg intraperitoneally (i.p) to animals of all the groups except animals belonging to the control and vehicle groups. The NMU dose of 75 mg/kg i.p was given to the animals two times at 1^{st} and 63^{rd} days of experimental timelines in the present study. In these contexts, it should also be mentioned that dose levels (50 mg/kg –75 mg/kg), number of doses (1-3 times) and administrating time intervals (6 - 9 weeks) of the NMU were found to be different from each other in quite a large studies on the NMU-induced

View Article Online
DOI: 10.1039/C5RA23005E

cancerous animal models as reported in literature.[28-34] After the NMU administration, treatments regime of the groups were as follows: animals of the diseased group received only usual food and water throughout the experiments; animals of the standard group received 20 mg/kg dose of Tamoxifen every alternative day throughout the course of the experiments; similarly, the low-dose, medium-dose and high-dose groups received the HDNB at concentration of 8 mg/kg, 40 mg/kg and 200 mg/kg (the doses were calculated based on results obtained from the AOT studies), respectively. At end of the experimental timeline, blood samples (serum and plasma) and breast tissues from all 6 animals of each group were collected, processed and preserved as per standard procedures. The samples were then subjected to hematology, histopathology, biochemical and immunohistochemical analysis and outcomes of the studies have been described in the following sections.

It is worthy of mentioning that all animals used in the chemopreventive studies were survived for the whole period of 18 weeks and the animals did not develop any toxic symptoms such as tremors, convulsions, salivation, diarrhea, lethargy, sleep and coma as inferred from protocols used to monitor the animals in a systematic manner (refer to Methods). The body weights of the different experimental groups were also monitored in regular intervals for 18 weeks and average body weights of animals belonging to seven different groups i.e. from Group I to VII were found to be 186 ± 3 g, 187 ± 2 g, 188 ± 4 g, 190 ± 4 g, 187 ± 3 g, 189 ± 5 g and 188 ± 5 g, respectively. There were no significant differences in the body weights between the HDNB-treated groups and any other groups (control/vehicle/standard/diseased groups) as determined from ANOVA (Analysis of Variance) statistical analysis of the data. Moreover, these results suggested that dose levels of the HDNB used in the chemopreventive studies did not cause any apparent behavioral changes and as well toxic symptoms to the animal models.

View Article Online
DOI: 10.1039/C5RA23005E

2.3.2 Histopathological analysis of breast tissues

All six Wistar rats of the control group showed no abnormality in cellular architectures of their breast tissue sections (Fig. 4A). Animals of the vehicle group also showed that there were no abnormalities in their breast tissues as compared to that of control group indicating the vehicle (corn oil) did not cause any adverse effect to the animals. On contrary, histopathological results clearly confirmed developments of mild dysplasia in the breast tissues of all six animals belonging to the diseased group (Fig. 4B) and the observations are in line with the literature reports on the NMU-induced cancerous animal models.[35,36] Interestingly, 20%, 80% and 50% of rats belonging to Group IV (low-dose group), Group V (medium-dose group) and Group VI (high-dose group), respectively showed breast tissues as similar as to that of control group. It is also worthy of mentioning that the rest of 80% rats in Group IV were characterized to have mild dysplasia in their breast tissues, while the rest of 20% and 50% of rats in Group V and Group VI depicted basophilia in alveolar and ductal epithelium. In the standard group, breast tissues of 50% of rats were found to be normal and rest of them were found to have basophilia in alveolar and ductal epithelium. Thus, the histopathological results suggested that the medium-dose (40 mg/kg b.w.) of the HDNB exhibited significant chemopreventive potential by suppressing abnormal cell proliferation occurring in the NMU-induced breast carcinoma of female Wistar rats (Fig. 4C).

2.3.3 Analyses of hematological parameters

Hematology studies were carried out to investigate alterations that may occur in standard levels of WBC (white blood cells) count, lymphocytes, neutrophils, monocytes, eosinophil, basophils, RBC (red blood cells) count and Hb (hemoglobin) of the animal models used in the present studies. The results of the studies have been enumerated in Table 2. The data revealed

View Article Online
DOI: 10.1039/C5RA23005E

that the diseased group showed two-fold increase of WBC, lymphocytes and neutrophils as compared to that of control group. From a review of data in Table 2, it is interesting to note that values of the hematological parameters of the medium-dose and high-dose groups showed no statistically significant differences to that of control group implying levels of WBC, lymphocytes and neutrophils could be restored in these groups as compared to the diseased group. Moreover, there were no significant differences between the medium/high dose groups and standard group with respect to these parameters. The same trend was also observed in the case of basophils of animal models, while eosinophils showed no significant alterations among all the seven groups. Concentration of hemoglobin, RBC and monocytes were found to be decreased in the diseased group relative to that of the control group. Though there were no statistically significant differences between all the 3 HDNB-treated groups and standard group with respect to these parameters, the medium-dose group restored the hemoglobin, RBC and monocytes in a noteworthy manner as compared to that of other 2 groups.

Taken together, remarkably decreased levels of RBC and increased levels of lymphocytes in Wistar rats of the diseased group are indications of developing anemia and lymphocytosis, respectively in those animal models. These types of inflammatory responses have also been reported in animals with mammary carcinoma as demonstrated in literature.[37, 38] In these contexts, the results described above are in line with those literature reports. In addition, development of leukaemia in the NMU-administered rats was also evidenced as per a few reports in the literature.[39, 40] Interestingly, the present study suggested that oral administration of the HDNB (40 mg/kg b.w.) brought back the status of WBC, RBC, lymphocytes and Hb to near normal range in the NMU-treated Wistar rats (Group V).

View Article Online
DOI: 10.1039/C5RA23005E

2.3.4 Analyses of biochemical end-products

Biochemical end-products such as total protein, albumin, creatinine, urea, alanine transferase (ALT), aspartate transferase (AST), gluthathione reductase (GR) and glutathione-S-transferase (GST) in blood serum/plasma were used to assess biological effect of the HDNB in the NMU-induced mammary carcinogenesis. Table 3 enumerates levels of these biochemical parameters as estimated using standard assays (refer to Methods) for all seven different experimental Wistar groups of the present study. The status of total protein and albumin were significantly decreased in Wistar rats of the diseased group comparing to that of the control group. Oral administration of medium dose of the HDNB (40 mg/kg b.w.) to the NMU-induced Wistar rats (Group V) significantly restored status of the total protein and albumin to near values of the respective parameters estimated for the control group (Table 3).

Aspartate transferase (AST) and alanine transferase (ALT) are generally being used as hepatic markers and significant alterations of these markers in blood plasma are probable indications of liver dysfunction and/or liver damage. The levels of AST and ALT were found to be significantly increased and decreased, respectively in the diseased group as compared to that of the control group. Among the low-, medium- and high-dose groups, Wistar rats of medium-dose group depicted AST and ALT levels, which were in good agreement with that of the control/standard groups (Table 3). These results indicated that the HDNB could restore liver functions by probably interfering with metabolic activations in the NMU-treated Wistar rats. The concentration of urea and creatinine, which serve as markers to examine renal functions, showed no significant alterations among all the seven experimental Wistar groups studied in the present study (Table 3). It should be mentioned that neither the hepatic markers nor renal markers mentioned above were abnormally estimated in both medium-dose and high-dose groups (Group

View Article Online
DOI: 10.1039/C5RA23005E

V & VI) suggesting 18 weeks oral administration of the HDNB at the dose concentration (40/200 mg/kg b.w.) in the NMU-induced mammary Wistar rats did not cause any severe adverse effects on the liver and kidney tissues. These findings lend credence to the reports from the AOT studies on the HDNB demonstrated in previous section of the work.

The GST and GR are phase II detoxification enzymes and they have been shown to be significantly altered in cancerous animal models.[41] The GST is reported to actively play critical roles in antioxidant defense mechanisms and detoxification of electrophilic/hydrophobic chemical compounds.[42] The enzyme is also known to be an important pre-neoplastic marker in assessing the carcinogen-induced free radical damage.[43] The GR is a critical cellular antioxidant enzyme which regulates the intracellular ratio of oxidized and reduced glutathione level.[44] While increased levels of the GST and GR facilitate excretion of carcinogenic metabolites either by conjugation with reduced glutathione or by destroying the reactive centers of carcinogen, activities of the enzymes are shown to be drastically decreased in cancerous animal models comparing that of healthy counterparts.[45, 46] In the present study, activations of both enzymes were significantly decreased in the diseased group as compared to that of the control group and the results corroborate the literature reports discussed above. Oral administration of medium-dose HDNB increased the GST and GR concentration on par with the standard drug, tamoxifen used in the present study, for bringing back the status of the enzymes to near normal range in blood plasma (Table 3). The data thus imply that the HDNB is capable of restoring the phase II detoxification enzymes and consequently stimulating excretion of carcinogenic metabolites that may be generated in the NMU-induced mammary carcinogenesis.

View Article Online
DOI: 10.1039/C5RA23005E

2.3.5 Analyses of lipid peroxidation and antioxidant markers

Oxidative stress occurring due to imbalance between oxidant and antioxidant levels plays pivotal roles in various stages of carcinogenesis.[47] Overproduction of reactive oxygen species (ROS) under the oxidative stress causes damages to biomacromolecules such as nucleic acids, proteins and lipids and subsequently altering cellular architectures and proliferations. Thus, end-products of oxidative stress, especially lipid peroxidation (oxidative degradation of lipids) byproducts such as malondialdehyde (MDA), tumor necrosis factor – alpha (TNF-α) and nitic oxide are considered as markers in many inflammatory diseases and as well in cancers.[48, 49] The MDA affects DNA functions by forming DNA-MDA adduct and TNF-α plays an important role in tumor progression by promoting expression of matrix metalloproteinases (MMP) and endothelial adhesion molecules to produce DNA damage.[50, 51] While NO (Nitric Oxide) acts as an antioxidant at low level, it is capable of damaging DNA at elevated concentrations and as well inducing alterations in cell functions to stimulate cell growth.[52, 53] In contrast, antioxidants play a major role in safeguarding the cells against the free radical induced toxicity. Hence, homeostasis of antioxidants and pro-oxidants are vital for normal cellular functioning and impairment in the balance would trigger the patho-physiological events causing damages to vital organs.[54-56]

In the present study, abnormalities of lipid peroxidation byproducts such as MDA, TNF-α and NO and as well antioxidant markers such as superoxide dismutase (SOD), catalase, glutathione peroxidase (GPx), reduced glutathione (GSH), vitamin C and vitamin E have been analyzed in blood samples of the experimental Wistar animal models. The status of MDA, TNF-α and NO were found to be significantly elevated in the diseased group comparing to that of the control group and the results are in conformity to lipid peroxidation effect on cancerous animal models reported in the literature.[49, 57] A comparative analysis of the status of the lipid

View Article Online
DOI: 10.1039/C5RA23005E

peroxidation byproducts in the HDNB-treated groups and diseased group revealed that low-dose group showed no significant changes, whereas both medium-dose and high-dose groups showed significant variations (Table 4). Of the two groups, the medium-dose group depicted better significant variations than the high-dose group as compared to the diseased group with respect to levels of the MDA, TNF-α and NO in those animal models. Moreover, there were no significant differences between estimated values of the parameters from the medium-dose group and the control/standard group indicating elevated levels of the MDA, TNF-α and NO were reversed to the normal levels in the NMU-induced Wistar mammary carcinogenesis upon subjecting the animal models to the HDNB medium-dose (40 mg/kg b.w.) treatments for 18 weeks.

Concentration of enzymatic antioxidants such as catalase, SOD and GPx and non-enzymatic antioxidants such as reduced glutathione and vitamin C were found to be significantly declined in the diseased group as compared to that of the control group. However, there were no significant changes in the status of vitamin E between the control group and other six groups (Table 4) implying metabolic activations in the NMU-treated Wistar rats had no effect on vitamin E status of blood plasma as inferred from the present study. However, significantly decreased level of vitamin E from the reference range was demonstrated in several animal models possessing cancer diseases due to chemical carcinogens as reported in the literature [58] and further discussion on the discrepancy is beyond the scope of this present study. Comprehensive analysis of the data on enzymatic and non-enzymatic antioxidants (GSH and vitamin C) obtained from the control and other six experimental groups revealed following information: both types of antioxidants could not be restored in low-dose HDNB-treated Wistar rats; though the antioxidants could be restored near to reference levels in both medium/high-dose HDNB-treated Wistar rats, efficacy of the medium-dose was found to be more satisfactory on reversing the

View Article Online
DOI: 10.1039/C5RA23005E

antioxidants levels near to the standard/control ranges than that of high-dose group (Table 4). Lowered levels of the antioxidants in blood plasma of the diseased group could presumably be due to excess amount of antioxidants utilizations by cancerous tissues either to meet their nutrient demand or to scavenge excessively generated reactive oxygen species.[59] In general, SOD removes the superoxide radical by converting it to hydrogen peroxide and molecular oxygen, whereas catalase decomposes hydrogen peroxides to water and dioxygen and as well protects tissues from the highly reactive hydroxyl radicals.[60, 61] The antioxidant glutathione peroxidase (GPx) plays an important role in peroxyl scavenging and as well maintaining the integration of the cell membranes.[62] Non-enzymatic antioxidants like reduced glutathione (GSH), vitamin C and vitamin E are acting as a second line defense agents to scavenge residual free radicals eluding from primary defense mechanisms by enzymatic antioxidants. As demonstrated above, oral administration of the medium-dose HDNB (40 mg/kg b.w.) to the NMU-treated Wistar rats was found to restore the antioxidants and lipid peroxidation byproducts to the level of the control group suggesting the HDNB may probably prevent cancer progression in the animal models by restoring the biomarkers scavenging the free radicals and consequently protecting cellular architectures. Strikingly, it is also obvious to note from the studies that the capabilities of the HDNB on restoring the antioxidants could supersede the standard drug, tamoxifen, used in the present study (Table 4).

2.3.6 Immunohistochemical studies on cancer biomarkers

Modulating effect of the HDNB on expression pattern of cell proliferative markers (Ki-67, p53) and as well an apoptotic (Bcl-2) marker have been investigated and described herein. Overexpression of Ki-67 in all proliferating cells is reported in the literature. Moreover, overexpression of Ki-67 in more than 50% of the breast cancer cells have been shown to be at

View Article Online
DOI: 10.1039/C5RA23005E

high risk of recurrent disease and thus it is also considered as a specific biomarker of breast cancers.[63-65] Tumor suppressor gene, p53 plays an important role in the prevention of cancers by inducing apoptosis, DNA repair and cell-cycle arrest in response to different types of cellular stress.[66] However, mutated forms of the p53 were shown to conferring a proliferative advantage to the neoplasm. Overexpression and as well active roles of p53 mutants have been well documented in various cancer types including breast carcinoma.[67, 68] Bcl-2, an anti-apoptotic protein, promotes cell survival by inhibiting apoptosis and the protein is well characterized to be overexpressed in various cancers, including breast cancer.[69] In general, all six anti-apoptotic proteins characterized to date are considered as crucial biomarkers as they are shown to be overexpressed in most of cancers, if not all, though overexpression pattern of each anti-apoptotic protein is unique with respect to cancer types. Overexpression of the anti-apoptotic proteins in cancer is due to impairment of apoptosis regulating a delicate balance of the pro-apoptotic and anti-apoptotic proteins.[70]

Immunohistochemical studies carried out on detecting the three molecular markers, Ki-67, p53 and Bcl-2 in breast tissues of female Wistar rats belonging to the diseased group apparently revealed overexpression of the markers. Immunostaining of proliferative markers Ki-67 and p53 variants and an apoptotic marker, Bcl-2 for the diseased group are depicted in Fig. 5B, Fig. 5E and Fig. 5H, respectively and overexpression of the molecular markers are represented by ‘arrow’ symbols in the respective pictorial illustrations. Abnormal expression patterns of the three molecular biomarkers in the female Wistar rats of the diseased group in the present study are in line with literature reports on status of the markers in animal models of different types of carcinogenesis.[65, 67, 71] Oral administration of the HDNB at a dose of 40 mg/kg b.w. to the NMU-treated Wistar rats significantly restored the three molecular markers to near

View Article Online
DOI: 10.1039/C5RA23005E

normal levels (Fig. 5C, 5F & 5I). Expression patterns of the Ki-67, p53 and Bcl-2 in the breast tissues of the control group are also shown for sake of comparison in Fig 5A, 5D & 5G, respectively. This particular efficaciousness of the HDNB on restoring the expressions of the molecular markers to normalcy justifies not only the protective effect of the HDNB in the NMU-induced Wistar mammary carcinogenesis and as well supports that the HDNB is a promising lead molecule to be developed as an efficient anti-cancer drug in near future.

3. Concluding remarks

In the present study, 2-hydroxy-3,5-dinitro benzamide (HDNB), a chemical compound identified by means of peptidodynmimetic computational approach, was synthesized and structurally characterized by using molecular spectrometric techniques such as UV, FT-IR, GC-MS, 1D and 2D NMR. To our best knowledge, biological properties of the compound have not yet been well documented in the literature. We have herein demonstrated the anti-cancer effect of the HDNB in animal models. The AOT studies suggested that LD_{50} of the compound must be at least greater than 2000 mg/kg b.w. The biological roles of the HDNB in NMU-induced Wistar mammary carcinogenesis were assessed by systematically analyzing the levels of various hematological parameters (WBC, RBC, Hb, lymphocytes, monocytes, neutrophils, basophils and eosinophils), biochemical end products (total protein, albumin, creatinine, urea ALT, AST, GST and GR), lipid peroxidation byproducts (MDA, TNF-α and NO), antioxidants (vitamin C, vitamin E, GSH, catalase, SOD and GPx), proliferative markers (Ki-67 and p53) and an apoptotic molecular marker (Bcl-2) by using established procedures. Medium-dose (40 mg/kg b.w.) of the HDNB showed appreciable potential to reverse the abnormalities of various biochemical parameters in blood samples and as well in breast tissue samples to the values as close as to that of the control/standard (Tamoxifen) groups. The chemopreventive effect of the

View Article Online
DOI: 10.1039/C5RA23005E

HDNB could be primarily attributed to its ability of restoring antioxidants and as well apoptosis inducing properties during the NMU-induced mammary carcinoma in Wistar animal models. The above results suggest that the HDNB is a promising seed molecule for developing prototypic chemical inhibitors to the anti-apoptotic proteins by using computational strategies such as 'core hopping' and *de novo* drug designing approaches in near future.[14, 25]

4. Materials and Methods

4.1 Chemicals

Thionyl chloride, 3,5-dinitrosalicylic acid (DNSA), liquid ammonia (ammonium hydroxide solution), tetrahydofuran (THF), dimethyl sulfoxide (DMSO), deuterium oxide (D_2O), N-nitroso-N-methyl urea (NMU) were obtained from Sigma-Aldrich chemicals Pvt. Ltd., Bangalore, Karnataka, India. Corn oil (brand name - Avita R-gold) was purchased from J.S. oils, Thanjavur, TamilNadu, India. 2,4-dinitrophenylhydrazine (DNPH), Folin-Ciocalteau reagent, 5,5'-dithiobis (2-nitro benzoic acid) (DTNB), trichloroacetic acid (TCA), hydrogen peroxide, heparin, phosphate buffer, reduced glutathione, epinephrine, ethylenediamine tetra-acetic acid (EDTA), 1-chloro-2,4 dinitro benzene (CDNB), thiobarbituric acid (TBA), diphenyl-1,10 phenonthroline, griess reagent, sodium nitroprusside were purchased from Hi-media laboratories, Mumbai, Maharashtra, India. P53, Ki-67 and Bcl-2 primary antibodies and corresponding secondary antibodies conjugated with horseradish peroxidase were purchased from Dako, Carprinteria, CA, USA. All the other chemicals/solvents used in the present study were also of analar grade.

4.2 Synthesis of the 2-hydroxy-3,5-dinitrobenzamide (HDNB)

A mixture of 3,5-dinitro salicylic acid (16.3 g, 0.05 mol) and thionyl chloride (120 ml) was refluxed with constant stirring until the suspension mixture was converted into a clear

View Article Online
DOI: 10.1039/C5RA23005E

solution. Excess amount of thionyl chloride added to the mixture was then removed under reduced pressure. The acid chloride of the parent compound obtained upon cooling was immediately dissolved in dry tetrahydrofuran (THF) and the resultant solution was added dropwise manner into a fresh ammonia solution kept in ice bath (≈ 273 K) with constant stirring. Target compound, 2-hydroxy-3,5-dinitro benzamide (HDNB), was formed as yellow precipitate in the reaction mixture. The HDNB was filtered (using Grade 1 Whatman paper), excessively washed with double distilled water to remove the acid impurity and then was dried in vacuum oven at 353 K. The HDNB was a bright yellow solid (5.7 g, 35% yield).

4.3 Structural characterizations of the HDNB

4.3.1 UV Spectroscopy

Absorption spectra of the HDNB and DNSA were recorded at 298 K in the wavelength range from 400 nm to 550 nm using double beam Lambda25 UV/Vis spectrophotometer (PerkinElmer, Wellesley, USA). The compounds were dissolved in DMSO and concentrations were 1.5 mM for both test solutions. Scan speed and slit width were set as 100 nm/minute and 1 nm, respectively. Absorption spectra for the compounds were also appropriately corrected to solvent effect.

4.3.2 FT-IR Spectroscopy

FT-IR spectra of the HDNB and DNSA were recorded on a Spectrum one FT-IR spectroscopy (PerkinElmer, Wellesley, USA). Sample preparation was carried out by thoroughly mixing HDNB/DNSA and KBr in the ratio of 1:3 (w/w) and pellet of the sample mixture was made using hydraulic press. Percentage of transmittances of the test samples was measured at scan speed of 0.2 cm/second and then the data were Fourier-transformed to generate spectra (covering wave number from 400 to 4000 cm^{-1}) with resolution of 2 cm^{-1}. FT-IR (KBr, cm^{-1}) for

View Article Online
DOI: 10.1039/C5RA23005E

the DNSA: 824, 1534, 1677, 2442, 2516, 2596, 2854, 2925, 3104 & 3448. FT-IR (KBr, cm^{-1}) for the HDNB: 805, 1564, 1602, 3135 & 3446.

4.3.3 GC-MS analysis

Molecular mass of the HDNB was determined by using Clarus 500 GC-MS (PerkinElmer, Wellesley, USA). Elite-5MS capillary Column (5% Phenyl, 95% dimethylpolysiloxane) of 30 meter in length was used at 453 K. 2 µL of the HDNB dissolved in DMSO at concentration of 1mg/100 µL (about 44 mM) was used for the analysis. Helium gas was used as carrier gas and flow rate was maintained as 1ml/minute. Sample could be fragmented and ionized by using electron energy of 70 ev in 'Electron Ionization' mode. Mass range for detecting various fragments of the HDNB upon electron bombardment was set to be from 20 to 600 amu. Total ion chromatogram of the HDNB showed two fragment species depicting molecular mass of 44 Da and 184 Da and the generated mass/charge data were used to search against NIST 2005 library in order to identify the structures of the HDNB (refer to supplementary material).

4.3.4 ^{1}H, ^{13}C and ^{15}N NMR studies

One dimensional ^{1}H NMR ($1D\ ^{1}H$ NMR) studies for the DNSA and HDNB dissolved in DMSO-d_6 were carried out using a 300 MHz AVANCE II (Bruker Biospin, Fallanden, Switzerland) NMR spectrometer equipped with a 5 mm BBO probe. Sample concentration was 2 mM in both cases. $1D\ ^{1}H$ NMR spectra for the test samples were acquired using zg30 standard pulse sequence with a relaxation delay of 1.0 sec at 298 K (temperature of the probe was calibrated using methanol standard[72]) and the acquired time domain data were then processed by Topspin 1.3 program. $1D\ ^{1}H$ NMR data of the HDNB dissolved in DMSO-d_6:D_2O solvents mixture (3:1, v/v) was also acquired at identical conditions as mentioned above. In all the $1D\ ^{1}H$

View Article Online
DOI: 10.1039/C5RA23005E

NMR experiments, tetramethylsilane (TMS) was used as an internal standard for referencing chemical shifts of various protons of the DNSA and HDNB. DEPT and two-dimensional HSQC-^{15}N experiments for HDNB were carried out using a 400 MHz NMR spectrometer equipped with a 5 mm AutoSW probe (Agilent Technologies, CA, USA). Default standard parameter settings of the programs as defined in the standard pulse sequence library of VnmrJ 2.2C were used except the following acquisition parameters: transients and t_1 increments were set as 4 and 512, respectively, for recording the HSQC spectrum; transients and a relaxation delay were set as 1024 and 1 second, respectively, for recording DEPT spectrum. TMS and CH_3NO_2 were used as internal standards for referencing chemical shifts of ^{13}C and ^{15}N resonances of the HDNB, respectively. ^{1}H NMR (300 MHz, DMSO-d_6) of the HDNB: δ 8.65 (s, 1H, CH), 8.70 (s, 1H, CH); DEPT ^{13}C NMR (400 MHz, DMSO-d_6) of the HDNB: δ 125.9, 131.5; HSQC - ^{15}N (400 MHz, DMSO- d_6) of the HDNB: δ 358.1; ^{1}H NMR (300 MHz, DMSO-d_6) of the DNSA: δ 8.67 (s, 1H, CH), 8.71 (s, 1H, CH).

4.4 In vitro cytotoxicity potential of the HDNB by MTT assay

The cancer cell lines (MG-63, MCF-7 and HeLa) were purchased from National Centre for Cell Science (NCCS), Pune, India and were grown in Eagles Minimum Essential Medium (EMEM), supplemented with 10% (v/v) fetal bovine serum (FBS) at 37 °C in a 5% CO_2 atmosphere. The monolayer cells were detached with trypsin-ethylene diamine tetra acetic acid (EDTA) to make single cell suspensions and viable cells were counted by trypan blue exclusion assay using a hemocytometer. The cell suspensions were seeded in 96-well plates at a density of 1 x 10^4 cells/well and treated with serial concentrations (ranging from 0.2 to 1000 µM) of the HDNB dissolved in neat DMSO. The plates were then incubated for an additional 48 h at 37 °C in a 5% CO_2 atmosphere. After the incubation, 15 µl of MTT (3-[4,5-dimethylthiazol-2-yl]2,5-

View Article Online
DOI: 10.1039/C5RA23005E

diphenyltetrazolium bromide) dissolved at concentration of 5 mg/ml in phosphate buffered saline (PBS) was added to each well and the plates were further incubated for another 4 h. Formazan crystals formed were solubilized in 100 µl DMSO and absorbance was measured at 570 nm using a microplate reader. The medium containing without the HDNB was served as control and all the experiments were performed in triplicate. The percentage of cell inhibition caused by the HDNB was determined using standard procedure[73] and the data were analysed by using GraphPad Prism software 5.01 (GraphPad Software, CA, USA).

4.5 Acute oral toxicity studies

A total of 5 Wistar female rats of about 8 weeks old with average weight of 175 ± 5 g were used as test animals for the acute toxicity studies and the animals were housed in standard polypropylene cages. Temperature, relative humidity and lighting of animal room were maintained at 25 ºC, 30-70% and 12/12 light/dark cycles, respectively throughout the experiments. The rats were provided with rodent laboratory diets (M/s Provimi Pvt. Ltd., Bangalore, Karnataka, India) and potable water purified by reverse osmosis *ad libitum*. The studies on the Wistar rats were conducted at Animal House, SASTRA University, using protocols approved by the Institutional Animal Ethics Committee of SASTRA University (CPCSEA – Committee for the Purpose of Control and Supervision of Experiments on Animals, Ministry of Environment and Forest, Government of India - ethical clearance for the animal studies is 227/SASTRA/IAEC/RPP).

Acute toxicity of the HDNB was tested in the animal models using 'Main test' procedure as per the OECD guidelines 425.[74] The HDNB was dissolved in corn oil and various doses (175 mg/kg, 550 mg/kg and 2000 mg/kg b.w.) of the compound were administrated using an oral gavage needle to the rats. It should be mentioned that single ordered dose progression wherein

View Article Online
DOI: 10.1039/C5RA23005E

the rats were dosed one at a time, at a minimum of 48 h intervals was followed and volume of doses was constantly maintained to be 1 ml irrespective of dose levels (dose progression factor was 3.2) and body weights of animals. Apparent changes on the physical systems and behavior patterns of the test animals were keenly noticed every 30 minutes for first 6 h and thereafter the animals were periodically monitored every 12 h for the experimental time span of 14 days. After 14 days, all the experimental animals were sacrificed and gross necropsies were done to examine any abnormalities or lesions in the internal organs such as brain, heart, lungs, liver, kidney and intestines.

4.6 In vivo studies using Wistar rats

A total of 42 female Wistar rats of about 8 weeks old with average body weight of 180 ± 6 g were used as test animals for the *in vivo* studies and the animals were housed in standard polypropylene cages. Temperature, relative humidity and lighting of animal room were maintained at 25 ºC, 30-70% and 12/12 light/dark cycles, respectively throughout the experiments. The rats were provided with rodent laboratory diets (M/s Provimi Pvt. Ltd., Bangalore, Karnataka, India) and potable water purified by reverse osmosis *ad libitum*. The 42 female Wistar rats were divided into seven groups (Group I – VII) and each group was consisted of six animals. The total study period was set as 18 weeks and doses (saline/corn oil/HDNB/Tamoxifen) were administered to animals belonging to various groups at every alternate day throughout the study period as mentioned below herein. Wistar rats of Group I served as ‘control group’ and the rats received only physiological saline as an oral dose throughout the experimental period. Group II rats received only vehicle (1ml of corn oil was orally given using stainless steel ball tipped oral intubation needle) and acted as ‘vehicle group’. Rats in groups III to VII were subjected to induction of mammary carcinogenesis by providing

View Article Online
DOI: 10.1039/C5RA23005E

intraperitoneal injection of 75 mg of NMU at 1st and 63rd days of the experiments. The carcinogen was freshly prepared prior to administration by dissolving it in 1ml of physiological saline. Group III rats received no other treatments throughout the experiments and hence the rats were considered as 'diseased group'. Group IV, V and VI rats were orally administered with the HDNB at concentration of 8 mg/kg (low-dose), 40 mg/kg (medium-dose) and 200 mg/kg (high-dose), respectively. The HDNB doses were also freshly prepared by suspending the finely grinded compound in corn oil, and the dose volume was adjusted to 1ml with plain corn oil in all cases. The low/medium/high doses of the HDNB were orally administered to rats of Group IV, V and VI using stainless steel ball tipped oral intubation needle. Group VII rats were orally administered with tamoxifen citrate (20 mg/kg body weight, dissolved in 1 ml of physiological saline) every alternate day and the dose was continued till the end of experimental timeline and the group served as 'standard group'.

4.6.1 Histopathology

At end of the study period, the rats were killed using CO_2 inhalation euthanasia and breast tissues and other organs of each animal were dissected out. All tissues were preserved in 10% neutral buffered formalin (NBF). The preserved breast tissues were then cut into thinner section (2-3 mm thick); processed using automatic Leica tissue processor TP 1020 (Leica Biosystems, Illinois, USA); embedded in paraffin wax using Leica EG 1150 H&C Embedding machine (Leica Biosystems, Illinois, USA) and cut into 3-4 μm sections using Leica RM 21° RTS (Leica Biosystems, Illinois, USA), which were mounted on clean glass slides. The sections of the tissues were stained with hematoxylin for 10 minutes followed with 0.5% eosin for another 5 minutes. The sections were then rapidly rinsed in 95% ethanol and dehydrated in absolute ethanol for 5 minutes using Leica ST 4040 Linear automatic stainer (Leica Biosystems,

View Article Online
DOI: 10.1039/C5RA23005E

Illinois, USA). Histological studies were carried out for the breast tissues of 6 animals from each group. A semi-quantitative grading scheme was used to evaluate the extent of the lesions in the tissues using five grades as follows: no lesion (grade 0); minimal (grade 1); mild (grade 2); moderate (grade 3); marked (grade 4) and severe (grade 5).[44, 45]

4.6.2 Haematological studies

Prior to necropsy of Wistar rats used in the *in vivo* experiments, blood samples were collected from the retro-orbital sinus of the rats in ethylene-diamine-tetraacetate (EDTA)-coated vials. The blood plasma was used for estimations of various hematological parameters by using 5 Part Mythic 22 Haematology AutoAnalyzer[75] (Orphee, Geneva, Switzerland).

4.6.3 Biochemical studies

Plasma was prepared from blood samples collected from the retro-orbital sinus of the experimental rats in the heparinized vials upon subjecting the blood samples to centrifugation at 1500 rpm for 10 min. After the centrifugation, the buffy coat was removed and the packed cells were washed thrice with physiological saline. The erythrocyte suspension was then prepared by the method of Dodge et al and modified by Quist.[76, 77] Similarly, serum was prepared by centrifuging the whole blood collected in sterile test tubes at 1500 rpm for 10 minutes. The resultant supernatant was collected and stored separately as described elsewhere.[78] Biochemical analysis were carried using the plasma/serum prepared from blood samples of 6 animals from each group and estimated values are expressed as mean ± standard error of the mean.

Lipid peroxide content was determined by thiobarbituric acid (TBA) reaction as assessed by Okhawa et al.[79] To the 0.5 ml of plasma, 1.5 ml of 20% acetic acid, 0.2 ml of sodium dodecyl sulphate (SDS) and 1.5 ml of TBA were added. The mixture was made up to 4.0 ml with distilled water and then heated for 60 minutes at 95° C using glass ball as condenser. After cooling to

View Article Online
DOI: 10.1039/C5RA23005E

room temperature, 4.0 ml of butanol-pyridine mixture was added, centrifuged and then absorbance was read at 532 nm. Standard and blank were treated in a similar manner. The lipid peroxide concentration was expressed as nmoles of malondialdehyde (MDA) formed/mg protein. The levels of tumor necrosis factor-α (TNF-α) was assayed by the method of Konturek et al.[80] The wells of microtiter plates were coated with 100 µL of blood plasma appropriately diluted in carbonate buffer. After incubating the plates at 4 °C for 12 h, 100 µL of serially diluted antibody was added and incubated at 37 °C for another 1 h. The wells were then charged with 100 µL of anti-rabbit IgG-conjugated with horseradish peroxidase (diluted 1:5000) at 37 °C for 1 h. The activity of bound horseradish peroxidase was monitored by addition of 50 µL of substrate (1 µL of hydrogen peroxide, 0.5 mg o-phenylenediamine (OPD) in 1 ml of citrate phosphate buffer, pH 5.0) at room temperature for 20 min in dark and the reaction was then arrested by adding 50 µL of 2 N sulfuric acid. The TNF-α concentration was recorded on ELISA (Enzyme-Linked Immunosorbent Assay) reader at 490 nm and expressed as ng/ml.

The extent of inhibition of nitric oxide radical generation *in vitro* was followed as per the method reported by Green et al.[81] The reaction was initiated by incubating mixture consisting of 2.0 ml of sodium nitroprusside, 0.5 ml of PBS and 0.5 ml of plasma at 25 °C for 30 minutes. Griess reagent (0.5 ml) was added to the mixture and incubated for another 30 minutes. The absorbance was read at 546 nm against the reagent blank (Genesys 10-S, USA) and the values were expressed as nmole/ml. The activity of catalase, superoxide dismutase (SOD) and Glutathione peroxidase in plasma were assayed by the method of Sinha, Misra & Fridovich and Rotruck et al with some modifications, respectively.[82-84] To 0.1 ml plasma, 0.9 ml of phosphate buffer and 0.4 ml of hydrogen peroxide were added and the reaction mixtures were kept in a boiling water bath for 10 minutes. The colour developed was read at 530 nm and the activity of

View Article Online
DOI: 10.1039/C5RA23005E

catalase was expressed as nmoles of H_2O_2 decomposed/min/mg protein. In case of SOD estimation, the plasma (0.5 ml) was mixed with 0.8 ml of carbonate buffer, 0.5 ml of EDTA solution and required amount of SOD. The reaction was initiated by the addition of 0.4 ml of epinephrine and the absorbance at 480 nm was measured. The enzyme activity was expressed as units/mg protein. For estimation of GPx, reaction mixture containing 0.4 ml buffer, 0.1 ml sodium azide, 0.2 ml reduced glutathione, 0.5 ml of plasma, 0.1 ml hydrogen peroxide and water was taken to a final incubation volume 2.0 ml at 30° C for 10 minutes. The reaction was terminated by the addition of 0.5 ml TCA. The supernatant prepared by centrifugation was mixed with 1.0 ml of DTNB reagent and the absorbance was measure at 412 nm. The GPx activity was expressed as nmoles of GSH utilized/min/mg protein.

The levels of reduced glutathione (GSH) were measured according to the method of Moron et al.[85] To 0.5 ml of plasma, 125 µL of 25 % TCA was added and centrifuged at 10,000 rpm for 10 minutes. Various aliquots of the supernatant were made up to 1 ml with 0.2 M sodium phosphate buffer (pH 8.0) and then mixed with 2.0 ml of freshly prepared DTNB solution. After incubation for 10 minutes at room temperature, the yellow colour formed was read at 412 nm. The levels of GSH were expressed as nmoles/mg protein. The method of Kyaw was adopted to estimate plasma ascorbic acid (vitamin C) content.[86] Absorbance of the supernatant prepared from the mixture consisting of 0.2 ml of plasma and 2 ml of colouring reagent was read at 700 nm and the value of vitamin C was measured as mg/dL of plasma. The method of Palan et al was adopted to estimate plasma alpha tocopherol (vitamin E) content.[87] To 0.5 ml of plasma, 1.5 ml of ethanol was added, mixed, centrifuged and the supernatant obtained was treated with 0.2 ml of bathophenanthroline reagent, 0.2 ml of ferric chloride reagent and 4 ml of butanol. The colour developed was read at 536 nm and the values of vitamin E were expressed as mg/dL of plasma.

View Article Online
DOI: 10.1039/C5RA23005E

4.6.4 Immunohistochemical studies

The immunohistochemical studies were carried out for cancer biomarkers such as Ki-67, p53 and Bcl-2. Breast tissues fixed in paraffin block as described earlier were deparaffinized by washing in xylene thrice and rehydrated by immersing in 95 % ethanol for 5 minutes followed by washing in distilled water. Endogenous peroxidase was blocked by incubation with 3% H_2O_2 in methanol for 10 minutes. The antigen retrieval was achieved by microwave in citrate buffer solution (2.1 g citric acid/L distilled water; 0.37 g EDTA/L distilled water; 0.2 g Trypsin; pH 6.0) for 10 minutes, followed by washing with Tris-buffered saline (8 g NaCl; 0.605 g Tris; pH 7.6). The tissue section was than incubated with ultra V block (protein block, Thermoscientific, USA) for 10 minutes at room temperature to block non-specific binding sites. The tissue sections were then incubated with the respective primary antibody (Ki-67, p53 and Bcl-2 – Dako, CA, USA) for 45 minutes at 4 °C and the bound primary antibody was detected by incubation with the secondary antibody conjugated with horseradish peroxidase polymer quanto (Thermoscientific, Massachusetts, USA) for 20 minutes at room temperature. After that, the slides were thoroughly rinsed with PBS and then the antigen-antibody complex was detected using 3,3'-Diaminobenzidine (DAB) quanto chromogen (Thermoscientific, Massachusetts, USA), the substrate of horseradish peroxidase. The slides were then washed, counterstained with haematoxylin for 10 sec and analyzed using optical microscope.

4.7 Statistical analysis

The values of hematology and biochemical results were expressed as mean ± SE (standard error). The statistical comparisons were performed by one-way ANOVA followed by Tukey's posthoc test for multi-group comparisons. Differences among the groups were

View Article Online
DOI: 10.1039/C5RA23005E

considered to be statistically significant only if a probability level was found to be lower than 5% ($p < 0.05$). The statistical analysis was performed using Graphpad Prism 5 software package.

Acknowledgements

The authors express sincere thanks to Mr. Biswajit Gorai for his expert assistance on performing animal experiments carried out in the present study and also 'Central Instrumentation facility of SASTRA' for generous support to conduct spectrometric studies (UV, FT-IR, GC-MS and 1D NMR) reported in the paper.

View Article Online
DOI: 10.1039/C5RA23005E

Abbreviations used in the text

Three-dimensional (3D); Alanine transferase (ALT); Analysis of variance (ANOVA); Acute oral toxicity (AOT); Aspartate transferase (AST); 1-chloro-2,4 dinitro benzene (CDNB); Committee for the purpose of control and supervision of experiments on animals (CPCSEA); Deuterium oxide (D_2O); 3,3'-Diaminobenzidine (DAB); Distortionless enhancement by polarization transfer (DEPT); Dimethyl sulfoxide (DMSO); 2,4-dinitrophenylhydrazine (DNPH); 3,5-Dinitiro salicylic acid (DNSA); 5,5'-dithiobis (2-nitro benzoic acid) (DTNB); Ethylenediamine tetra-acetic acid (EDTA); Enzyme-linked immunosorbent assay (ELISA); Eagles minimum essential medium (EMEM); Fetal bovine serum (FBS); Fourier transform infrared (FT-IR); Gas chromatography - mass spectrometry (GC-MS); Glutathione peroxidase (GPx); Gluthathione reductase (GR); Reduced glutathione (GSH); Glutathione-S-transferase (GST); Hemoglobin (Hb); human Bax-BH3 (hBax-BH3); human Bcl-B (hBcl-B); 2-hydroxy-3,5-dinitrobenzamide (HDNB); Heteronuclear single quantum correlation (HSQC); Lethal dose (LD_{50}); Malondialdehyde (MDA); Matrix metalloproteinases (MMP); 3-[4,5-dimethylthiazol-2-yl]2,5-diphenyltetrazolium bromide (MTT); Neutral buffered formalin (NBF); National centre for cell science (NCCS); N-Nitroso-N-methylurea (NMU); Nuclear magnetic resonance (NMR); Nitric oxide (NO); Organization for economic cooperation and development (OECD); o-Phenylenediamine (OPD); Phosphate buffered saline (PBS); Red blood cells (RBC); Reactive oxygen species (ROS); Sodium dodecyl sulphate (SDS); Superoxide dismutase (SOD); Thiobarbituric acid (TBA); Trichloroacetic acid (TCA); Tetrahydofuran (THF); Tetramethylsilane (TMS); Tumor necrosis factor – alpha (TNF-α); Ultraviolet visible (UV); White blood cells (WBC).

View Article Online
DOI: 10.1039/C5RA23005E

References

1 M. Guo, B.A. Hay, *Curr. Opin. Cell Biol.,* 1999, **11**, 745–752.

2 R.J. Duronio, Y. Xiong, *Cold Spring Harb. Perspect. Biol.,* 2013, **5**, a008904.

3 S. Fulda, K-M. Debatin, *Oncogene.,* 2006, **25**, 4798-4811.

4 G. Lessene, P.E. Czabotar, P.M. Colman. *Nat. Rev. Drug Discov.,* 2008, **7**, 989-1000.

5 J.C. Reed, *Nat. Rev. Drug Discov.,* 2002, **1**, 111-121.

6 I. Marzo, J. Naval, *Biochem. Pharmacol.*, 2008, **76**, 939-946.

7 J.E, Chipuk, D.R. Green, *Trends. Cell. Biol.* 2008, **18**, 157-164.

8 H. Kim, M. Rafiuddin-Shah, H.C. Tu, J.R. Jeffers, G. Zambetti, J.J.D. Hsieh, E.H.Y. Chang, *Nat. Cell. Biol.* 2006, **8**, 1348-1358.

9 S.N. Willis, J.I. Fletcher, T. Kaufmann, M.F. van Delft, L. Chen, P.E. Czabotar, H. Ierino, E.F. Lee, W.D. Fairlie, P. Bouillet, A. Strasser, R.M. Kluck, J.M. Adams, D.C. Huang, *Science*, 2007, **315**, 856-859.

10 P.N. Kelly, A. Strasser, *Cell Death Differ.*, 2011, **18**, 1414-1424.

11 T. Oltersdorf, S.W. Elmore, A.R. Shoemaker, R.C. Armstrong, D.J. Augeri, B.A. Belli, M. Bruncko, T.L. Deckwerth, J. Dinges, P.J. Hajduk, M.K. Joseph, S. Kitada, S.J. Korsmeyer, A.R. Kunzer, A. Letai, C. Li, M.J. Mitten, D.G. Nettesheim, S. Ng, P.M. Nimmer, J.M. O'Connor, A. Oleksijew, A.M. Petros, J.C.Reed, W. Shen, S.K. Tahir, C.B. Thompson, K.J. Tomaselli, B. Wang, M.D. Wendt, H. Zhang, S.W. Fesik, S.H. Rosenberg, *Nature*, 2005, **435**, 677-681.

12 C. Tse, A.R. Shoemaker, J. Adickes, M.G. Anderson, J. Chen, S. Jin, E.F. Johnson, K.C. Marsh, M.J. Mitten, P. Nimmer, L. Roberts, S.K. Tahir, Y. Xiao, X. Yang, H. Zhang, S. Fesik, S.H. Rosenberg, S.W. Elmore, *Cancer Res.* 2008, **68**, 3421-3428.

View Article Online
DOI: 10.1039/C5RA23005E

13 D. Yecies, N.E. Carlson, J. Deng, A. Letai, *Blood*, 2010, **115**, 3304-3313.

14 D. Sivakumar, B. Gorai, T. Sivaraman, *Mol. BioSyst.,* 2013, **9**, 700-712.

15 D. Sivakumar, N. Hari, T. Sivaraman, *Bangladesh J. Pharmacol.,* 2014, **9**, 307-311.

16 J.A. Prescher, C.R. Bertozzi, *Nat. Chem. Biol.,* 2005, **1**, 13-21.

17 S.L. Schreiber, *Nat. Chem. Biol.,* 2005, **1**, 64-66.

18 J.A. Wells, C.L. McClendon, Nature., 2007, **450**, 1001-1009.

19 A.W. White, A.D. Westwell, G. Brahemi, *Expert Rev. Mol. Med.,* 2008, **10**, e8.

20 S. Lise, C. Archambeau, M. Pontil, D.T. Jones, *BMC Bioinformatics.,* 2009, **10**, 365-382.

21 P. Vanhee, A.M. van der Sloot, E. Verschueren, L. Baeten, F. Stricher, L. Serrano, F. Rousseau, J. Schymkowitz, *Trends Biotechnol.*, 2011, **29**, 231-239.

22 M. Floris, J. M. Masciocchi, M. Fanton, S. Moro, *Nuc. Acids Res.,* 2011, **39**, W261-269.

23 M.J. Strauss, *Ind. Eng. Chem. Prod. Res. Dev.* 1979, **18**, 158-166.

24 G. Liu, W.K. Kelly, G. Wilding, L. Leopold, K. Brill, B. Somer, *Clin. Cancer Res.,* 2009, **15**, 3172-3176.

25 D. Sivakumar, T. Richa, S.S. Rajesh, B. Gorai, T. Sivaraman, *Mini-Rev. Med. Chem.,* 2012, **12**, 1144–1153.

26 J.F. Hardisty, S.L. Eustis, in Progress in predictive toxicology, ed. D.B. Clayson, I.C. Munro, P. Shubik, J.A. Swenberg, Elsevier, New York, 1990, Toxicological pathology: A critical stage in study interpretation, 41.

27 WHO. Principles and methods for evaluating the toxicity and chemicals. Part I. in: Environmental Health Criteria 6. World Health Organization, 1978, pp.192.

28 N.B.V. Barbosa, C.W. Nogueira, T.N. Guecheva, M.L. Bellinaso, J.B.T. Rocha, *Arch. Toxicol.,* 2008, **82**, 655-633.

View Article Online
DOI: 10.1039/C5RA23005E

29 A.K. Smolarek, J.Y. So, B. Burgess, A.T. Kong, K. Reuhl, Y. Lin, W.J. Shih, G. Li, M-J. Lee, Y-K. Chen, C.S. Yang, N. Suh, *Cancer Prev. Res.,* 2012, **5**, 1310-1320.

30 K. Christov, C.J. Grubbs, A. Shilkaitis, M.M. Juliana, R. A. Lubet, *Clin. Cancer. Res.,* 2007, **13**, 5488-5496.

31 I. Vegh, R.E. Salamanca, *J. Carcinog.,* 2007, **6**, 18-26.

32 P. Kubatka, I. Ahlers, E. Ahlersova, E. Adamekova, P. Luk, B. Bojkova, M. Markova, *Cancer Lett.,* 2003, **202,** 131-136.

33 R. A. Lubet, D. Boring, V.E. Steele, J. M. Ruppert, M.M. Juliana, C.J. Grubbs, *Cancer Prev Res.,* 2009, **2**, 161-167.

34 J. Liska, S. Galbavy, d. Macejova, J. Zlatos, J. Britko, *Endocrine Regulations*, 2000, **34**, 91-96.

35 S. Golbabapour, W.W. Pang, J. George, T. Pasupati, P.S. Abdul-Rahman, O.H. Hashim, *Int. J. Mol. Sci.,* 2011, **12**, 1030-1040.

36 M. W. Roomi, N.W. Roomi, V. Ivanov, T. Kalinovsky, A. Niedzwiecki, M. Rath, *Breast Cancer Res.,* 2005, **7**, R291-R295.

37 M. Perse, A. Cerar, R. Injac, B. Strukelj, *Pathol. Oncol. Res.,* 2009, **15**, 115–121.

38 H. Hazilawati, A.H. Hutheyfa, S.M. Rosly, S. Jasni, M.M. Noordin, S. Shanmugavelu, *Med. J. Malaysia.,* 2010, **65**, 125-126.

39 R. Saffhill, L. Chaudhuri, *Nucl. Acids Res.,* 1976, **3**, 277–284.

40 Y.C. Chang, J.D. Hsu, W.L. Lin, Y.J. Lee C.J. Wang, *Arch. Toxicol.,* 2012, **86**, 315–327.

41 C. di Ilio, P. Sacchetta, G. del Boccio, G. la Rovere, G. Federici, *Cancer Lett.,* 1985, **29**, 37–42.

42 J.D. Hayes, D.J. Pulford, *Crit.Rev. Anal. Chem.,* 1995, **30**, 445-520.

View Article Online
DOI: 10.1039/C5RA23005E

43 D.J. Reed, *CAnn. Rev. Pharmacol. Toxicol.,* 1990, **30**, 603-631.

44 X. Liu, S.J. Sturla, *Mol. Biosyst,,* 2009, **5,** 1013-1024.

45 S. Manoharan, S. Balakrishnan, V.P. Menon, L.M. Alias, A.R. Reena, *Singapore Med. J.,* 2009, **50**, 139–146.

46 C. Kumar, A. Igbaria, B. D'Autreaux, A.G. Planson, C. Junot, E. Godat, A.K. Bachhawat, A. Delaunay-Moisan, M.B. Toledano, *EMBO. J.,* 2011, **30**, 2044–2056.

47 H. Sies, *Exp. physiol.,* 1997, **82**, 291–295.

48 F. Nielsen, B.B. Mikkelsen, J.B. Nielsen, H.R. Andersen, P. Grandjean, *Clin. Chem.,* 1997, **43**, 1209–1214.

49 I. Vegh, R.E. de Salamanca, Prolactin, *J. Carcinog.,* 2007, **6**, 18–26.

50 L.J. Marnett, *Mutat. Res.*, 1999, **424,** 83–95.

51 K. Fehsel, V. Kolb-Bachofen, H. Kolb, *Am. J. Pathol.,* 1991, **139,** 251–254.

52 H.T. Chung, H.O. Pae, B.M. Choi, T.R. Billiar, Y.M. Kim, *Biochem. Biophys. Res. Commun.*, 2001, **282,** 1075–1079.

53 T. deRojas-Walker, S. Tamir, H. Ji, J.S. Wishnok, S.R. Tannenbaum, *Chem. Res. Toxicol.,* 1995, **8,** 473–477.

54 J. Nordberg, E.S. Arnér, *Free Radic. Biol. Med.,* 2001, **31,** 1287–1312.

55 A. Rahal, A. Kumar, V. Singh, B. Yadav, R. Tiwari, S. Chakraborty, K. Dhama, *BioMed. Research International.,* 2014, **2014**, 1-19.

56 M. Valko, C.J. Rhodes, J. Moncol, M. Izakovic, M. Mazur, *Chemico-Biol. Inter.,* 2006, **160,** 1–40.

57 J.L. Wang, D. Liu, Z.J. Zhang, S. Shan, X. Han, S.M. Srinivasula, C.M. Croce, E.S. Alnemri, Z. Huang, *Proc. Natl. Acad. Sci. USA.,* 2000, **97,** 7124–7129.

View Article Online
DOI: 10.1039/C5RA23005E

58 S. Manoharan, S. Balakrishnan, V.P. Menon, L.M. Alias, A.R. Reena, *Singapore Med. J.* 2009, **50,** 139–146.

59 H. Magdelenat, Breast cancer advances in biology and therapeutics, John Libbey Eurotext, Paris, 1996, 63.

60 B.H. Robinson, *Biochim. Biophys. Acta.,* 1998, **1364,** 271–286.

61 A.L. Brioukhanov, A.I. Netrusov, *Biokhimiia.*, 2004, **69,** 949–962.

62 R. Chandra, R. Aneja, C. Rewal, R. Konduri, S.K. Dass, S. Agarwal, *Ind. J. Clin. Biochem.,* 2000, **15,** 155–160.

63 A.P. Locker, K. Birrell, J.A, Bell, R.I. Nicholson, C.W. Elston, R.W. Blamey, I.O. Ellis, *Eur. J. Surg. Oncol.* 1992, **18,** 224–229.

64 L. Assersohn, J. Salter, T.J. Powles, R. A'hern, R.K. Gregory, J. Chang, M. Dowsett, *Breast Cancer Res. Treat.,* 2003, **82,** 113–123.

65 G. Cattoretti, M.H. Becker, G. Key, M. Duchrow, C. Schluter, J. Galle, J. Gerdes, *J. Pathol.,* 1992, **168,** 357–63.

66 K. Bourougaa, N. Naski, C. Boularan, C. Mlynarczyk, M.M. Candeias, S. Marullo, R. Fahraeus, *Mol. Cell.,* 2010, **38,** 78–88.

67 A.K. Negi, S. Kansal, A. Bhatnagar, N. Agnihotri, *Tumour Biol.,* 2013, **34**, 3753–64.

68 E. Lim, F. Vaillant, D. Wu, N.C. Forrest, B. Pal, A.H. Hart, M.L. Asselin-Labat, D.E. Gyorki, Ward, T. Partanen, A. Feleppa, F. Huschtscha, L.I. Thorne, H.J. kConFab, S.B. Fox, M. Yan, J.D. French, M.A. Brown, G.K. Smyth, J.E. Visvader, G.J. Lindeman, *Nat. Med.,* 2009, **15,** 907–913.

69 S.J. Dawson, N. Makretsov, F.M. Blows, K.E. Driver, E. Provenzano, J. Le Quesne, L. Baglietto, G. Severi, G.G. Giles, C.A. McLean, G. Callagy, A.R. Green, I. Ellis, K. Gelmon,

View Article Online
DOI: 10.1039/C5RA23005E

G. Turashvili, S. Leung, S. Aparicio, D. Huntsman, C. Caldas, P. Pharoah, *Br. J. Cancer.,* 2010, **103**, 668–675.

70 N.N. Danial, S.J. Korsmeyer, *Cell*., 2004, **116**, 205–219.

71 K. Sahin, M. Tuzcu, N. Sahin, F. Akdemir, I. Ozercan, S. Bayraktar, O. Kucuk, *Nutr. Cancer.*, 2011, **63,** 1279–1286.

72 A.L. VanGeet, *Anal. Chem.,* 1970, **42**, 679-680.

73 A. Monks, D. Scudier, P. Skehan, R. Shoemaker, K. Paull, D. Vistica, C. Hose, J. Langley, P. Cronise, A. Vaigro-Wolff, M. Gray-Goodrich, H. Campbell, J. Mayo, M. Boyd, *J. Natl. Cancer Inst.,* 1991, **83**, 757-766.

74 OECD. Guidelines for testing of chemicals. Acute oral toxicity – up and down procedure. 2001, **425**, 1-26.

75 A.K. Wassmuth, B. Riond, R. Hofmann-Lehmann, H. Lutz, *J. Vet. Diagn. Invest.,* 2011, **23**, 436-453.

76 J.T. Dodge, C. Mitchel, D.J. Hanahan, *Arch. Biochem. Biophys.,* 1968, **100,** 119–130.

77 E.H. Quist, Regulation of erythrocyte membrane shape by calcium ion. *Biochem, Biophys. Res. Commun.,* 1980, **92**, 631–637.

78 M.K. Tuck, D.W. Chan, D. Chia, A.K. Godwin, W.E. Grizzle, K.E. Krueger, W. Rom, M. Sanda, L. Sorbara, S. Stass, W. Wang, D.E. Brenner, *J. Proteome. Res.,* 2009, **8,** 113-117.

79 H. Okhawa, N. Ohishi, K. Yagi, *Anal. Biochem.,* 1979, **95**, 351–357.

80 P.C. Konturek, T. Brzozowski, S.J. Konturek, S. Kwiecien, A. Dembinski, E.G. Hahn, *Scand. J. Gastroenterol.,* 2001, **36**, 1239-1247.

81 L.C. Green, D.A. Wagner, J. Glogowski, P.L. Skipper, J.S. Wishnok, S.R. Tannenbaum, *Anal. Biochem.,* 1982, **126**, 131–138.

View Article Online
DOI: 10.1039/C5RA23005E

82 A.K. Sinha, Colorimetric assay of catalase, *Anal. Biochem.*, 1972, **47**, 389-394.

83 H.P. Misra, I. Fridovich, *J. Biol. Chem.,* 1972, **247**, 3170-3175.

84 J.T. Rotruck, A.L. Pope, H. Ganther, A.B. Swanson, D.G. Hafeman, W.G. Hoekstra, *Science,* 1973, **179**, 588–590.

85 N.S. Moron, J.W. Depierr, B. Mannervik, *Biochem. Biophy. Acta.,* 1979, **582**, 67–72.

86 A. Kyaw, *Clinica. Chimica. Acta.,* 1978, **86,** 153–157.

87 P.R. Palan, B.S. Mikhail, J. Basu, S.L. Roomney, *Nutr. Cancer.,* 1973, **15,** 13–20.

View Article Online
DOI: 10.1039/C5RA23005E

Legends to Figures

Fig. 1 Structural characterizations of the HDNB as probed by NMR. (A) 1D ^{1}H NMR spectra of (A) DNSA, (B) HDNB and (C) HDNB in which labile protons were deuterated are shown. (D) 1D ^{13}C DEPT spectrum depicting two tertiary carbon resonances of the HDNB is shown and internal standard resonance of the spectrum is denoted as TMS. (E) ^{15}N-HSQC spectrum shows a cross peak for presence of an amide group in the HDNB.

Fig. 2 Effect of the HDNB on various organs of Wistar female rats subjected to AOT studies. (A) Brain section revealing normal appearing neurons (arrow) and neuropil (arrowhead). (B) Heart section showing normal myocytes (arrow) arranged in overlapping spiral patterns with no lesions. (C) Lung section with normal alveolar/bronchiolar epithelium (arrow). (D) Liver section with normal appearing hepatocytes (arrow) arranged as hepatic cords adjacent to hepatic sinusoids (arrowhead) showing no significant degenerative or inflammatory changes. (E) Kidney section with normal glomeruli (arrow) and tubules (arrow head) micro-architecture. (F) Intestinal section (colon) with normal appearing epithelium (arrow) showing no ulcerative lesions. All the organ sections were stained using Haematoxylin - Eosin (HE) stain. The reader is referred to web version of the article for color representation of the figure.

Fig. 3 *In vitro* cytotoxicity potential of the HDNB by MTT assay. Concentration-dependent inhibition potential of the HDNB against growth of MCF-7 (breast cancer cells), MG-63 (osteosarcoma cells) and HeLa (cervical cancer cells) cell lines.

Fig. 4 Histopathological studies of breast tissues of Wistar female rats belonging to various groups. A) Breast tissues of control group. B) Breast tissues of diseased group showing mild dysplasia. C) Breast tissues of medium-dose (40 mg/kg b.w.) group showing remarkably decreased levels of dysplasia and the tissues resemble as if that of normal cells (HE staining,

View Article Online
DOI: 10.1039/C5RA23005E

40X magnification). The reader is referred to web version of the article for color representation of the figure.

Fig. 5 Immunohistochemical studies of cancer biomarkers such as Ki-67, p53 and Bcl-2. Immunoexpression patterns of Ki-67, p53 and Bcl-2 in breast tissues of the diseased group are shown in B, E and H, respectively. Arrows indicate overexpressed Ki-67, p53 and Bcl-2 in the respective figures. There were no overexpression patterns for the Ki-67, p53 and Bcl-2 in the breast tissues of medium dose (40 mg/kg b.w.) group as shown in C, F and I, respectively. Expression patterns of the Ki-67, p53 and Bcl-2 in the breast tissues of control group are shown in A, D and G, respectively. The reader is referred to web version of the article for color representation of the figure.

View Article Online
DOI: 10.1039/C5RA23005E

Table 1 Various animal groups of chemopreventive *in vivo* experiments performed in the present study.

Experimental Groups	**Treatments***	**No. of Wistar rats**
Group I	Control Group (1 ml of saline)	6
Group II	Vehicle Group (1 ml of corn oil)	6
Group III	Diseased Group (75 mg NMU/kg b.w.)	6
Group IV	Low-dose group (8 mg HDNB/kg b.w.)	6
Group V	Medium-dose group (40 mg HDNB/kg b.w.)	6
Group VI	High-dose group (200 mg HDNB/kg b.w.)	6
Group VII	Standard Group (20 mg Tamoxifen/kg b.w.)	6

* Refer to method section for detailed explanation

View Article Online
DOI: 10.1039/C5RA23005E

Table 2 Various hematological parameters of blood samples collected from Wistar rats belonging to each of seven experimental groups (Group I – VII). Values of the parameters are represented as mean ± SE (n=6).

	Group I	Group II	Group III	Group IV	Group V	Group VI	Group VII
WBC (10^3/µl)	6.7±0.5	6.3±0.6	15.4±3.2	7.4±1.1*	5.8±1.7**	6.4±1.6**	7.0±0.1*
Lymphocytes %	69.4±2.4	73.4±2.9	151.6±4.3	149±10.9	65.8±4.6***	64.6±1.8***	76.3±13.5***
Neutrophils %	11.6±0.6	9.9±0.4	21.1±1.3	16.4±1.5*	10.3±0.4***	10.9±1.0***	11.4±0.6***
Monocytes %	3.3±0.4	2.6±0.3	2.6±0.2	2.7±0.3	3.2±0.4	2.9±0.2	3.1±0.1
Eosinophils %	2.4±0.1	2.1±0.1	2.3±0.01	2.1±0.02	2.0±0.01*	2.0±0.03	2.2±0.1
Basophils %	0.02±0.01	0.03±0.01	0.3±0.1	0.13±0.03	0.05±0.03**	0.1±0.01**	0.1±0.01**
RBC (10^6/µl)	7.5±0.2	7.5±0.2	5.4±0.4	7.9±0.3***	7.4±0.2**	7.7±0.1***	6.8±0.3*
Hb (g/dl)	13.7±0.5	12.8±0.9	12.0±0.6	14.3±0.3*	13.7±0.3	13.1±0.1	13.8±0.2

The '*' symbol denotes significant differences between the Group III and Group IV/V/VI/VII. Significantly different ($0.01 \leq P \leq 0.05$), very significantly different ($0.001 \leq P < 0.01$) and extreme significantly different ($P < 0.001$) data were denoted by *, ** and ***, respectively.

View Article Online
DOI: 10.1039/C5RA23005E

Table 3 Various biochemical end-products of blood samples collected from Wistar rats belonging to each of seven experimental groups (Group I – VII). Values of the parameters are represented as mean ± SE (n=6).

Parameters	**Group I**	**Group II**	**Group III**	**Group IV**	**Group V**	**Group VI**	**Group VII**
Protein (g/dl)	7.3±0.1	6.9±0.2	6.5±0.2	6.6±0.3	7.1±0.1**	6.9±0.1*	6.8±0.1
Albumin (g/dl)	4.1±0.1	4±0.1	3.6±0.2	3.9±0.2	4.33±0.1***	4.2±0.3**	3.7±0.1
Creatinine (mg/dl)	0.80±0.02	0.75±0.03	0.78±0.03	0.75±0.02	0.73±0.04	0.73±0.04	0.78±0.03
Urea (mg/dl)	51.8±1.6	49±1.8	47.8±1.8	52.5±1.1	47±1.4	47.8±1.3	53.5±1.5
ALT (IU/L)	52±1.2	53.7±0.9	44.7±1.2	54±1.5**	50.33±1.9	57.7±2.0***	52±1.2*
AST (IU/L)	196.3±7.9	200.7±0.9	276.5±6.6	245.7±8.1*	187.3±7.4***	191.7±5.8***	198±7.2***
GR (nmoles/min/mg)	35.9±0.5	34.2±1.9	22.5±0.6	19±0.2	32.66±1.4***	28.5±1.2*	30.1±1.8**
GST (nmoles/min/mg)	41.6±0.7	37±3.3	21.7±0.4	24.3±1.8	32.2±1.7*	30.3±1.7	31.0±3.8*

The '*' symbol denotes significant differences between the Group III and Group IV/V/VI/VII. Significantly different ($0.01 \leq P \leq 0.05$), very significantly different ($0.001 \leq P < 0.01$) and extreme significantly different ($P < 0.001$) data were denoted by *, ** and ***, respectively.

View Article Online
DOI: 10.1039/C5RA23005E

Table 4 Various biochemical end-products of blood samples collected from Wistar rats belonging to each of seven experimental groups (Group I – VII). Values of the parameters are represented as mean ± SE (n=6).

Parameters	**Group I**	**Group II**	**Group III**	**Group IV**	**Group V**	**Group VI**	**Group VII**
MDA (nmoles/mg)	1.3±0.1	1.4±0.1	2.4±0.1	2.3±0.3	1.55±0.01**	1.75±0.01*	1.7±0.1*
TNF-α (ng/ml)	3.3±0.4	3.2±0.1	5.9±0.4	6.3±0.6	3.3±0.2**	3.9±0.4*	5.8±0.3
NO (nmole/ml)	6.1±0.4	6.6±0.5	14.7±0.4	13.2±0.7	7.9±0.7***	8.9±0.9**	10.7±1.9*
CAT (nmoles/min/mg)	70.4±3.4	84±1.8	36.8±1.1	54.6±3.5**	73.1±1.0***	72.9±2.0***	52.8±2.8**
SOD (units/mg)	5.2±0.2	4.5±0.3	3±0.1	2.5±0.3	4.8±0.3**	3.5±0.5	4.6±0.01**
GPx(nmoles/min/mg)	39.2±1.9	34.3±2.1	22.9±1.3	23.5±1.9	36.57±1.2***	33.8±0.6**	25.8±1.8
GSH (nmoles/mg)	38.3±1.5	36.6±1.2	20.5±0.7	23.0±1.1	32.47±1.1***	32.8±2.2***	28.7±1.8**
Vit C (mg/dl)	1.6±0.01	1.1±0.2	0.77±0.01	0.9±0.01	1.2±0.1*	1.0±0.01	1.1±0.2
Vit E (mg/dl)	1.8±0.1	1.3±0.2	1.1±0.1	1.3±0.01	1.5±0.1	1.4±0.1	1.4±0.2

The '*' symbol denotes significant differences between the Group III and Group IV/V/VI/VII. Significantly different ($0.01 \leq P \leq 0.05$), very significantly different ($0.001 \leq P < 0.01$) and extreme significantly different ($P < 0.001$) data were denoted by *, ** and ***, respectively.

View Article Online
DOI: 10.1039/C5RA23005E

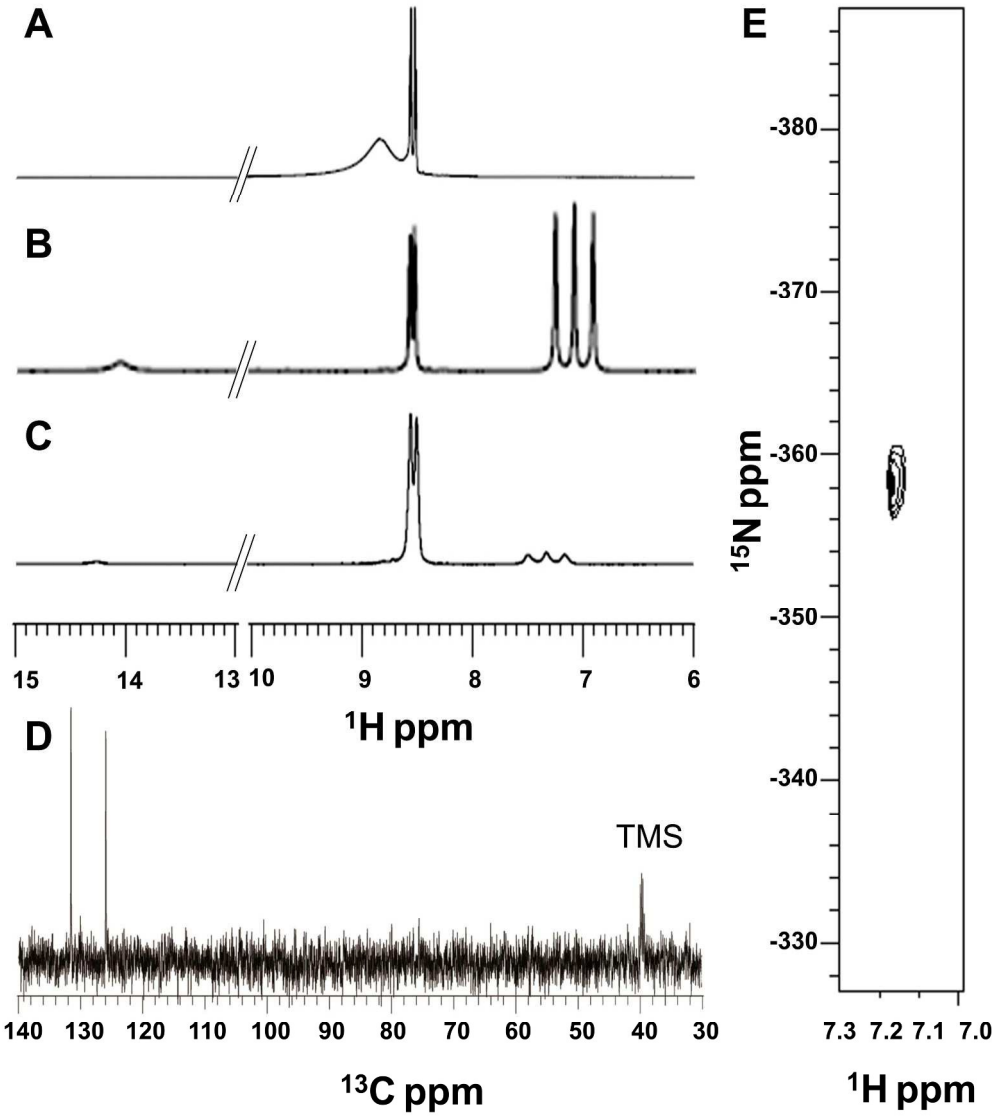

250x283mm (300 x 300 DPI)

View Article Online
DOI: 10.1039/C5RA23005E

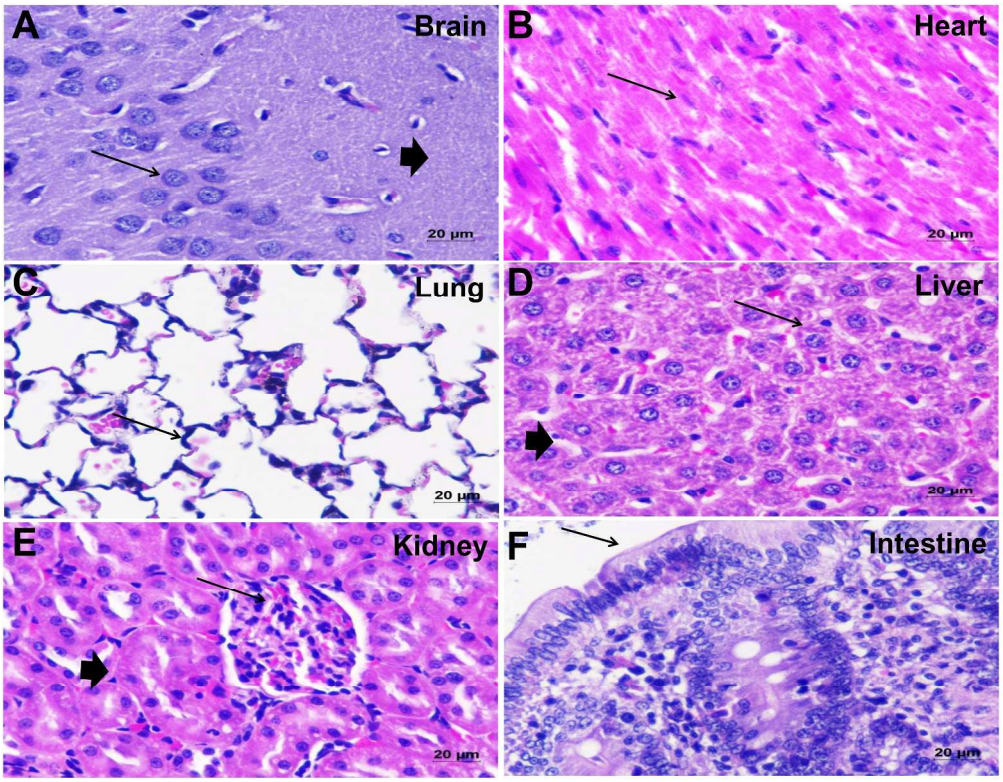

295x229mm (300 x 300 DPI)

View Article Online
DOI: 10.1039/C5RA23005E

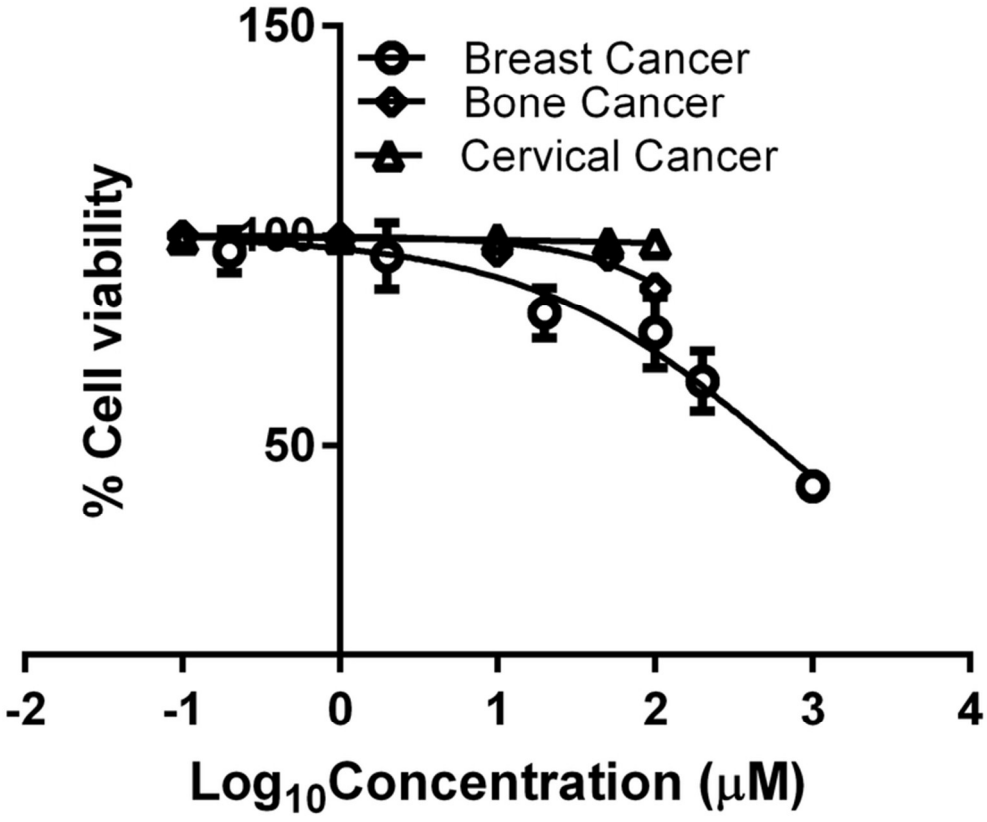

67x56mm (300 x 300 DPI)

View Article Online
DOI: 10.1039/C5RA23005E

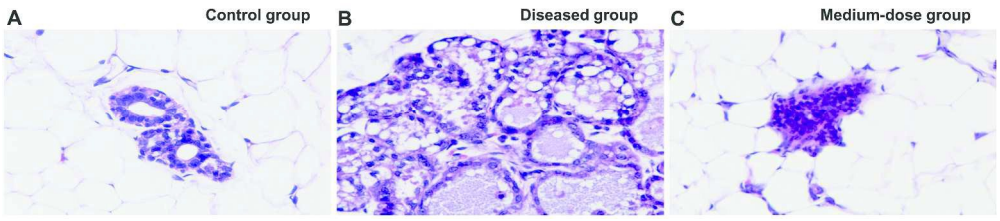

448x96mm (300 x 300 DPI)

View Article Online
DOI: 10.1039/C5RA23005E

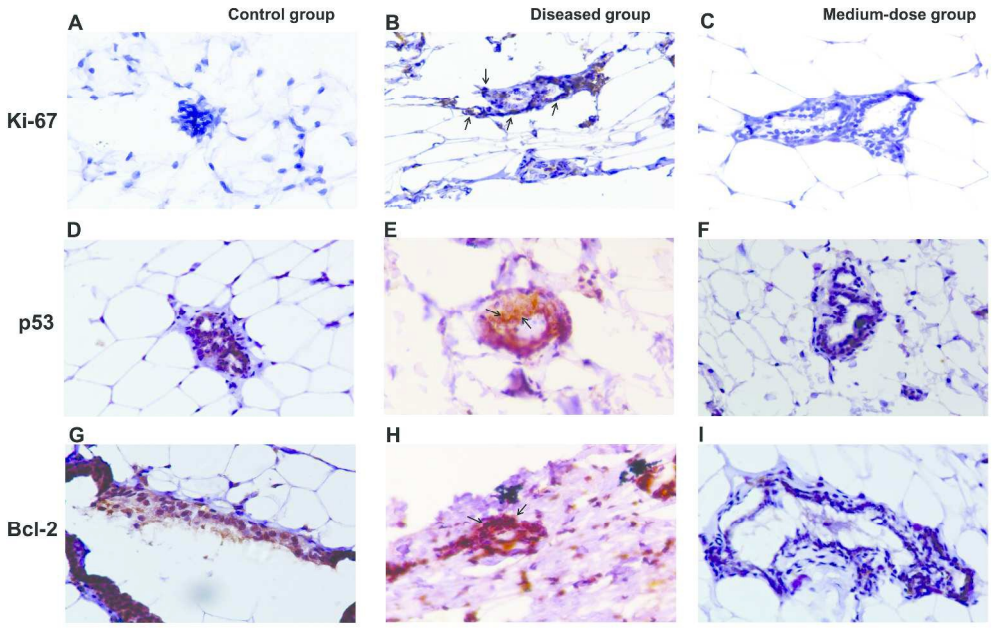

440x280mm (300 x 300 DPI)

View Article Online
DOI: 10.1039/C5RA23005E

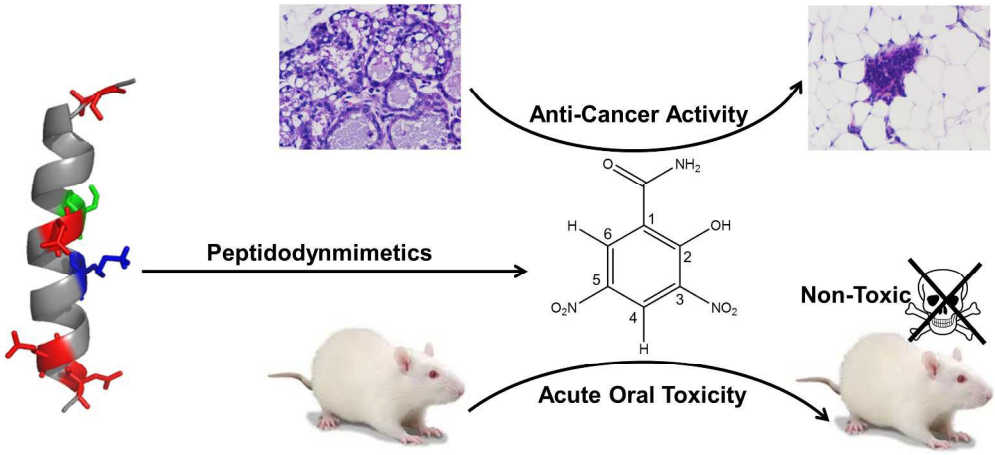

244x110mm (300 x 300 DPI)